Optics Letters

Resonant pumped erbium-doped waveguide lasers using distributed Bragg reflector cavities

G. Singh,[1,*] Purnawirman,[1] J. D. B. Bradley,[1] N. Li,[1,3] E. S. Magden,[1] M. Moresco,[1] T. N. Adam,[2] G. Leake,[2] D. Coolbaugh,[2] and M. R. Watts[1]

[1]Photonic Microsystems Group, Research Laboratory of Electronics, Massachusetts Institute of Technology, 77 Massachusetts Avenue, Cambridge, Massachusetts 02139, USA
[2]College of Nanoscale Science and Engineering, University at Albany, State University of New York, 257 Fuller Road, Albany, New York 12203, USA
[3]John A. Paulson School of Engineering and Applied Science, Harvard University, Cambridge, Massachusetts 02138, USA
*Corresponding author: gurpreet_singh@dsi.a-star.edu.sg

Received 29 December 2015; revised 2 February 2016; accepted 4 February 2016; posted 4 February 2016 (Doc. ID 256541); published 10 March 2016

This Letter reports on an optical pumping scheme, termed resonant pumping, for an erbium-doped distributed feedback (DFB) waveguide laser. The scheme uses two mirrors on either side of the DFB laser, forming a pump cavity that recirculates the unabsorbed pump light. Symmetric distributed Bragg reflectors are used as the mirrors and are designed by matching the external and internal quality factors of the cavity. Experimental demonstration shows lasing at an optical communication wavelength of around 1560 nm and an improvement of 1.8 times in the lasing efficiency, when the DFB laser is pumped on-resonance.

OCIS codes: (130.3120) Integrated optics devices; (140.3460) Lasers.

http://dx.doi.org/10.1364/OL.41.001189

Erbium-doped waveguide lasers [1] present several advantages for laser integration on a silicon photonics platform [2]. Such lasers permit monolithic integration [3], are compatible with low-cost complementary metal-oxide-semiconductor (CMOS) processes [4], and have been shown to achieve high-performance ultranarrow linewidths [5]. One underlying issue, however, is that, unlike fiber lasers [6], erbium-doped waveguide lasers are typically limited in pump absorption lengths, particularly because of their small footprint size. To allow sufficiently short pump absorption lengths, erbium-doped waveguide lasers are doped with higher levels of erbium concentrations [7], which can, however, lead to increase in energy transfer upconversions [8] and concentration-quenching effects [9]. Alternatively, pump recirculating schemes can be used to effectively increase the number of pump passes over a short length. For instance, a highly reflective mirror can be placed at the end of an erbium-doped waveguide laser and reflect the unabsorbed pump back into the laser [10]. This permits two pump passes but prevents dual-sided pumping, from the side of the highly reflective mirror. To allow multiple pump passes, an additional reflective mirror can be placed at the laser input, forming a pump cavity. Such a scheme has been discussed in [11], for erbium-doped fiber lasers.

In this Letter, we report on a multiple-pump-pass scheme, termed resonant pumping, for an erbium-doped distributed feedback (DFB) waveguide laser. By placing reflective mirrors on either side of the DFB laser, a pump cavity is formed where multiple pump passes can be sustained at resonant frequencies. We use symmetric distributed Bragg reflectors (DBRs) as reflective mirrors and an input pump diode with an optical wavelength matching a cavity resonance, at 976 nm. We demonstrate lasing at an optical communication wavelength of around 1560 nm and show that when pumped on-resonance, a 1.8 times improved lasing efficiency can be achieved.

In the integrated DFB laser and DBR pump cavity design, silicon nitride (SiN_x) layers are used to define the waveguide and grating features [4]. A layer of erbium-doped aluminum oxide (Al_2O_3:Er^{3+}) is deposited on top as a final process step, for producing gain. Figure 1(a) shows the top view (x–z plane) of the SiN_x layers that define the DFB laser and DBR pump cavity. A multisegmented SiN_x design is used to reduce the wavelength sensitivity of the overlaps between the laser and pump optical modes [3]. It is also used to maintain a high overlap within the gain region while maintaining a thick SiN_x for passive device integration [12]. The width of a single SiN_x segment is 0.6 μm, while the gap between them is 0.4 μm. The DFB laser (quarter-wave phase-shifted) consists of perturbations with a period of 0.487 μm, formed by placing stubs 0.5 μm away from the first and last SiN_x layers. The stub width is 0.4 μm. The DBR pump cavity is realized by placing DBR gratings on either side of the DFB laser. The grating perturbations have a period of 0.298 μm and are formed by etching out 0.1 μm from both sides of the center SiN_x layer. The center SiN_x has a width W_c of 0.458 μm. The lengths of the DBR grating and DFB laser are 350 μm and 2 cm, respectively. Some length exists between the ends of the DFB laser and the DBR gratings, and, hence, the total length of the DBR pump cavity is 2.11 cm. The integrated DFB laser and DBR pump cavity were fabricated in a standard CMOS foundry, with a fabrication process similar to that in [4]. The

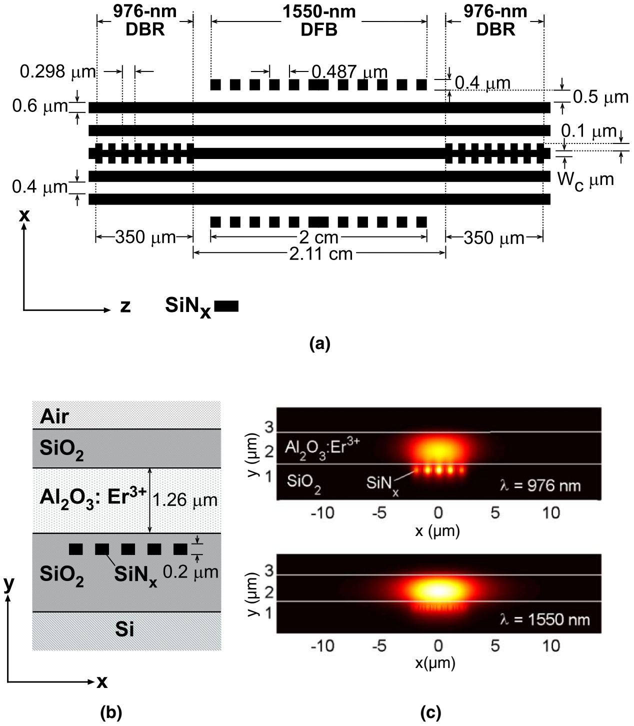

Fig. 1. Design of the resonantly pumped DFB laser: (a) top view of the SiN_x double-cavity structure showing 976 nm pump DBRs and the 1550 nm DFB. (b) Cross-sectional drawing of the composite waveguide structure. (c) Calculated intensity profiles of the 976 nm pump and 1550 nm laser modes.

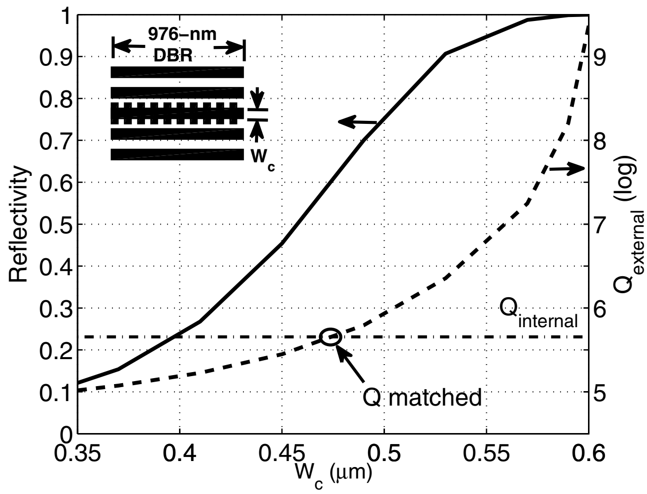

Fig. 2. Calculated 976 nm DBR grating reflectivity and corresponding external Q (dashed line) for different grating center widths W_c. The design width W_c is selected around the Q matching point.

cross-sectional view (x–y plane) is shown in Fig. 1(b). The thickness of the SiN_x layers and the SiO_2 gap are both 0.2 μm. The thickness of the Al_2O_3:Er^{3+} film is 1.26 μm, as measured using the prism coupling method [13]. A layer of index-matching fluid (SiO_2, $n = 1.45$) is placed on top of the laser during measurement, as will be discussed, subsequently. The intensity distributions of the fundamental TE mode for both the pump (976 nm) and laser (1550 nm) modes are shown in Fig. 1(c). Good laser–pump mode overlaps can be achieved owing to their similar intensity distributions.

The pump cavity DBR grating design was based on matching the grating external quality factor (Q) to the internal Q of the pump cavity, for critical coupling [14]. The internal Q was calculated from the total pump loss that consists of both the background loss in the Al_2O_3:Er^{3+} film and the erbium absorption loss. The background loss was measured to be 0.1 dB/cm [4]. The erbium absorption at 976 nm was calculated to be 0.91 dB/cm from the doping concentration of 1.5×10^{20} ions/cm^3, the measured absorption cross section of 2×10^{-21} cm^2 [15], and the pump confinement factor of 0.76. The total pump loss is thus 1.01 dB/cm. Using the total pump loss value and the effective index of 1.6353 at 976 nm, the internal Q can be calculated to be 4.53×10^5 (5.66 in log scale) [16]. The grating external Q was calculated using the following relation [16]:

$$Q = \frac{\omega}{\log\left(\frac{1}{R^2}\right)\frac{v_c}{2L}}, \tag{1}$$

where v_c is the phase velocity, L is the length of the cavity (2.11 cm), and R is the grating reflectivity, which was determined by the coupled-mode theory [17]. We assume symmetric gratings on either end of the cavity. Figure 2 plots the DBR reflectivity for different center widths W_c, on the left y axis. The corresponding external Qs are plotted on the right y axis (in log scale). From the plot in Fig. 2, we can deduce that the external Q matches the internal Q of 5.66 (plotted as a dashed–dotted line), when the center width W_c is about 0.47 μm. Following the grating design, transfer matrix calculations were performed to determine the amount of field enhancement produced by the cavity, at resonance. The amount of enhancement was calculated as the ratio between the field intensity in the cavity and the intensity in a single-pass case. This can be expressed at various points along the cavity as

$$\zeta(z) = \frac{|E_f(z) + E_r(z)|^2}{|E_{fs}(z)|^2}, \tag{2}$$

where $E_f(z)$ and $E_r(z)$ are the forward and backward propagating electric fields along the cavity, respectively, and $E_{fs}(z)$ is just the forward electric field in the single-pass case. A standing wave is formed in the cavity, with periodic maximum and minimum electric-field fluctuations. Figure 3(a) shows a contour plot of the maximum field enhancements for various cavity lengths and erbium doping concentrations. The maximum value was taken at the center of the cavity, where much of the DFB laser intensity exists. Note that these calculations assumed Q-matched grating reflectivities. Figure 3(b) further shows a contour plot of the average field enhancements, averaged throughout the pump cavity. It can be easily deduced that the enhancement increases as the cavity length shortens or the erbium concentration reduces. For a cavity length of 2.11 cm and an erbium doping concentration of 1.5×10^{20} ions/cm^3, the maximum and average field intensity enhancements are 2.7 and 1.5, respectively. We hence expect laser performance improvements, within this range, when pumped on-resonance.

To experimentally compare the lasing performance of the same DFB laser, under both on- and off-resonance pumping, we consider shifting the pump grating response by applying a layer of index-matching fluid on the laser. The input pump

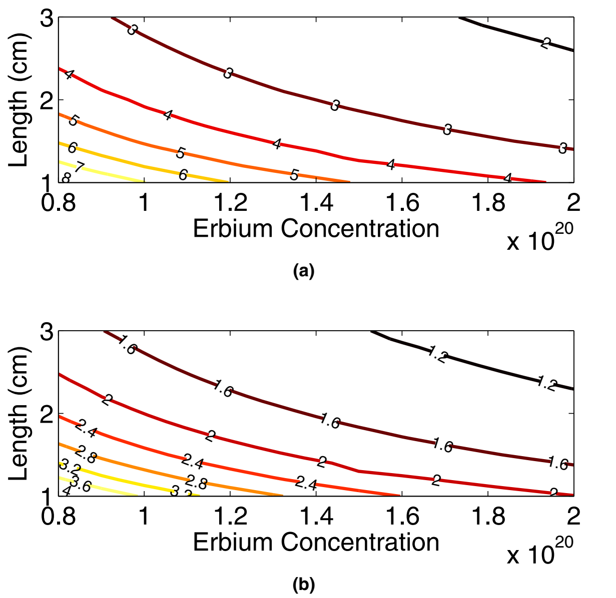

Fig. 3. Contour plot of the cavity-induced field enhancement for different cavity lengths and erbium concentrations (ions/cm^3): (a) maximum enhancement, (b) average enhancement.

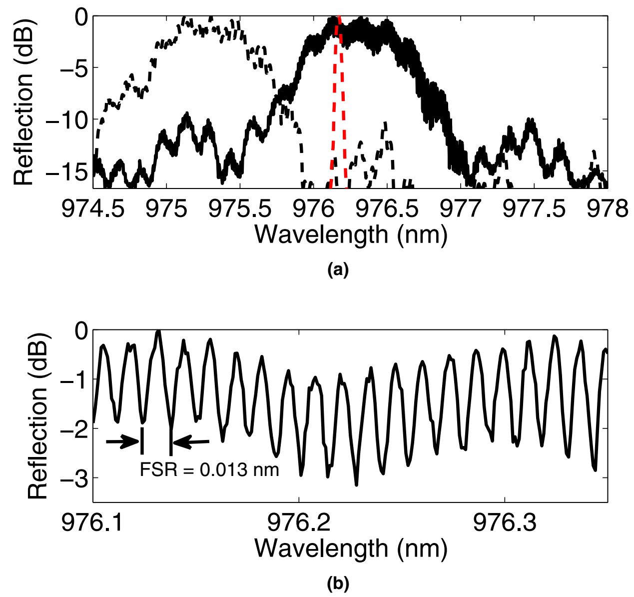

Fig. 4. Measured reflection (normalized) from the 976 nm pump cavity: (a) broad 976 nm grating response when shifted toward the pump (straight line), with the index-matching fluid on top, and away from the pump (dashed line), without the index-matching fluid on top. The red line plots the pump diode spectrum. (b) Zoomed-in view of fine cavity Fabry–Perot resonances. The FSR is 0.013 nm.

diode center wavelength is kept fixed at around 976.2 nm. Several other methods were considered such as heating/cooling the laser to shift the grating response and tuning the pump diode, instead, while keeping the grating response fixed. In the former approach, the amount of heating/cooling was not sufficient to tune the broad grating response of 1.3 nm. Furthermore, condensation was observed while cooling, which caused difficulty in pump coupling. In the latter approach, the tunability of a narrow-linewidth laser diode is relatively limited (around 0.1 nm) and tuning the pump wavelength can change the absorption cross sections. Applying an index-matching fluid on the laser can be an effective way to sufficiently tune the grating response (around 1 nm), although care should be taken to not change the laser cavity characteristics drastically. Table 1 shows the confinement factor (Γ) and grating strengths (κ), with and without the index-matching fluid on the laser cavity, at both the pump and signal wavelengths. The difference in confinement factor, between the cases of with and without the index-matching fluid, is small and not very significant, at both pump and signal wavelengths. The grating strength at the pump wavelength is almost the same, and, hence, any grating loss would be similar. The grating strength at the signal wavelength does reduce with the index-matching fluid. This would make it slightly harder to lase. The reason for a relatively similar laser cavity, between the cases of with and without the index-matching fluid, is because of a thick Al_2O_3:Er^{3+} film.

Table 1. Laser Cavity Characteristics With and Without Index-Matching Fluid on Top

	976Γ	1550Γ	976κ	1550κ
Without index matching	0.73	0.846	143.8/m	568.7/m
With index matching	0.76	0.850	144.5/m	502.6/m

Figure 4(a) shows the measured reflection (broad DBR grating response), with and without the index-matching fluid. With the index-matching fluid, the response shifts toward the input pump center wavelength. The grating bandwidth is 1.3 nm. Figure 4(b) shows a zoomed-in view of the measured reflection around the pump center wavelength, where very fine Fabry–Perot cavity resonances can be seen. The free-spectral range (FSR) of these resonances is 0.013 nm, which corresponds to the theoretical FSR of a 2.11 cm long cavity.

Figure 5 is the experimental setup used to measure the laser power from the integrated DFB laser and DBR pump cavity. An Innovative Photonics Solutions narrow-linewidth 976 nm pump diode (<1 MHz) is coupled onto the chip through a directly spliced isolator, a 980 nm polarization controller, and a 980/1550 nm wavelength-division multiplexer (WDM). Laser output is collected from the 1550 nm outputs of both the right and left WDMs, and measured using an optical spectrum analyzer. By insertion loss measurements, we estimate coupling losses per facet of 4.2 and 5.7 dB for 976 and 1550 nm, respectively, without the index-matching fluid on the chip. The coupling losses are 3.3 and 4.5 dB for 976 and 1550 nm, respectively, with the index-matching fluid. Figure 6(a) shows the lasing spectrum when the laser is pumped on-resonance. Lasing is observed at 1563 nm. Figure 6(b) shows the on-chip laser power versus the on-chip pump power for cases when the laser is pumped on- and off-resonance. From the plot, the slope efficiencies can be estimated to be 2.2% and 1.2% with on- and off-resonance pumping, respectively. An improvement of 1.8 times is thus achieved when the laser is pumped on-resonance. This improvement falls within the predicted enhancement ranges of 1.5 and 2.7, as discussed above. The 2.2% efficiency achieved, when pumped on-resonance, is comparable to, if not better than,

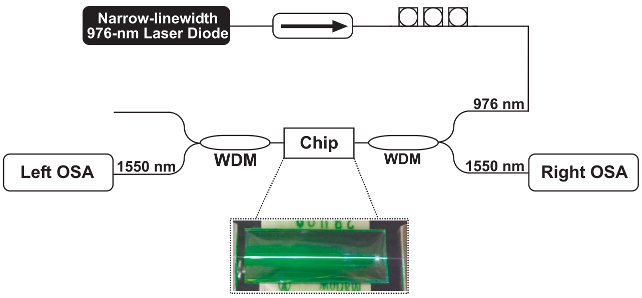

Fig. 5. Experimental setup used to characterize the resonantly pumped DFB laser.

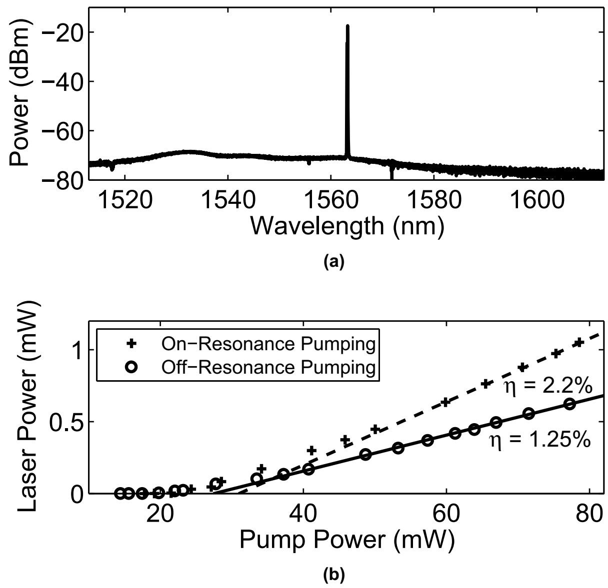

Fig. 6. DFB laser power measurement: (a) laser spectrum showing lasing at 1563 nm, when the laser is pumped on-resonance; (b) on-chip laser power versus on-chip pump power with on- and off-resonance pumping.

the efficiencies of 1.1% and 0.77% presented in [7] and [10], respectively, for an $Al_2O_3:Er^{3+}$ DFB laser pumped at 976 and 974 nm.

The current demonstration of a resonant pumped DFB laser sets up potentially interesting works in the future. Shorter laser cavities (<1 cm), which previously suffered from low pump absorption [18], can in the future be investigated with resonant pumping, to recirculate the pump light and improve the laser performance. The benefits of reducing the laser length include a smaller footprint size, a relatively even distribution of the pump light, and easier single-longitudinal-mode lasing [18]. Figures 3(a) and 3(b) show a possible enhancement of at least 2.5 times when the cavity length is reduced to 1 cm. If the erbium concentration is further reduced to 1.0×10^{20} ions/cm^3, the enhancement increases to 3.5 times. Several variations of resonantly pumped shorter laser cavities can be developed by working with varying laser lengths and erbium concentrations to achieve improved lasing performances. Similar pump cavity designs can be developed for DFB lasers pumped at 1480 nm and for DBR lasers pumped at both 980 and 1480 nm.

In summary, this Letter has demonstrated resonant pumping for an erbium-doped DFB laser. A pump cavity was formed by placing DBR gratings on either side of the DFB laser. The design of the DBR gratings was based on matching the internal and external *Qs*. Experimental measurements showed an improvement of 1.8 times in the lasing efficiency when the DFB laser was pumped on-resonance. The proposed resonant pumping scheme can be potentially useful for shorter laser cavities, which previously suffered from low pump absorption. Further efforts in designing shorter laser cavities with resonant pumping can be demonstrated in the future.

Funding. Defense Advanced Research Projects Agency (DARPA) (HR0011-12-2-0007).

REFERENCES

1. J. D. B. Bradley and M. Pollnau, Laser Photon. Rev. **5**, 368 (2011).
2. G. T. Reed, *Silicon Photonics: the State of the Art* (Wiley, 2008), pp. 147–189.
3. J. D. B. Bradley, E. S. Hosseini, Purnawirman, Z. Su, T. N. Adam, G. Leake, D. Coolbaugh, and M. R. Watts, Opt. Express **22**, 12226 (2014).
4. Purnawirman, J. Sun, T. N. Adam, G. Leake, D. Coolbaugh, J. D. B. Bradley, E. S. Hosseini, and M. R. Watts, Opt. Lett. **38**, 1760 (2013).
5. E. H. Bernhardi, H. A. G. M. van Wolferen, L. Agazzi, M. R. H. Khan, C. G. H. Roeloffzen, K. Worhoff, M. Pollnau, and R. M. de Ridder, Opt. Lett. **35**, 2394 (2010).
6. L. V. Kotov, M. E. Likhachev, M. M. Bubnov, O. I. Medvedkov, M. V. Yashkov, A. N. Guryanov, J. Lhermite, S. Fevrier, and E. Cormier, Opt. Lett. **38**, 2230 (2013).
7. E. H. Bernhardi, "Bragg-grating-based rare-earth-ion-doped channel waveguide lasers and their applications," Ph.D. dissertation (University of Twente, 2012).
8. E. S. Hosseini, Purnawirman, J. D. B. Bradley, J. Sun, G. Leake, T. N. Adam, D. D. Coolbaugh, and M. R. Watts, Opt. Lett. **39**, 3106 (2014).
9. L. Agazzi, K. Worhoff, and M. Pollnau, J. Phys. Chem. C **117**, 6759 (2013).
10. M. Belt and D. J. Blumenthal, Opt. Express **22**, 10655 (2014).
11. R. Waarts, "Resonant pumped short cavity fiber laser," U.S. patent 6,185,230 (February 6, 2001).
12. Purnawirman, E. S. Hosseini, A. Baldycheva, J. Sun, J. D. B. Bradley, T. N. Adam, G. Leake, D. Coolbaugh, and M. R. Watts, "Erbium-doped laser with multi-segmented silicon nitride structure," in *Optical Fiber Communication Conference* (Optical Society of America, 2014), paper W4E.5.
13. J. D. B. Bradley, L. Agazzi, D. Geskus, F. Ay, K. Worhoff, and M. Pollnau, J. Opt. Soc. Am. B **27**, 187 (2010).
14. H. A. Haus, *Waves and Fields in Optoelectronics* (Prentice-Hall, 1984), pp. 197–234.
15. L. Agazzi, K. Worhoff, A. Kahn, M. Fechner, G. Huber, and M. Pollnau, J. Opt. Soc. Am. B **30**, 663 (2013).
16. B. E. A. Saleh and M. C. Teich, *Fundamentals of Photonics* (Wiley, 1991), pp. 310–341.
17. T. Murphy, "Design, fabrication, and measurement of integrated Bragg grating optical filters," Ph.D. dissertation (MIT, 2001).
18. M. Belt, T. Huffman, M. L. Davenport, W. Li, J. S. Barton, and D. J. Blumenthal, Opt. Lett. **38**, 4825 (2013).